

## STUDY OF PROPERTIES OF NiTi ALLOY AFTER ELECTRON BEAM ZONE MELTING

MADAJ Michal, SZURMAN Ivo, DRÁPALA Jaromír, VONTOROVÁ Jiřina, POHLUDKA Martin

VSB - Technical University of Ostrava, Ostrava, Czech Republic, EU

### Abstract

The NiTi alloy was remelted by electron beam zone melting. The initial state of the NiTi samples was after swaging. After electron beam floating zone melting the samples were prepared for optical metallographic analysis, scanning electron microscopy analysis and EDX analysis. Next analysis was made to determine the concentration of interstitial elements (C, O, N). The obtained results were compared to NiTi alloys prepared previously by other technologies (centrifugal casting, etc.).

**Keywords:** NiTi alloy, electron zone melting, NiTi microstructure, Nitinol, SME

### 1. PROPERTIES AND FABRICATION OF NiTi BASED ALLOYS

What concerns the well-known Shape Memory Alloys (SMA), the most extensive investigation is devoted to an intermetallic compound with body centred cubic lattice called Nitinol, which is a NiTi based alloy. Its properties, such as good corrosion resistance and biocompatibility, make it an ideal material for biocompatible applications, such as orthodontic wires, stents or orthopaedic implants. This intermetallic compound is paramagnetic with low permeability at constant temperature range from 160 to 538 °C. The basic physical properties of NiTi based alloys are presented in **Table 1** [1, 2, 3].

**Table 1** Basic physical properties of equiatomic composition of NiTi based alloys [2]

Melting temperature of various equiatomic composition of NiTi based alloys (°C)	1992 - 2117
Density (kg/m <sup>3</sup> )	6449
Module of elasticity (GPa)	69.63
Module of rigidity (GPa)	26.20

The Shape Memory Alloy effect was discovered only for equiatomic composition of NiTi based alloy (i.e. 50 at.% of nickel and 50 at. % of titanium), specifically for the B2-phase, which exhibits maximal temperature of martensitic phase transformation of approx. 120 °C. Martensite phase obtained from twinning mechanism after transformation shows compatible crystallographic structure, which is changed in dependence on composition and transformation temperature between B2 structure for the base phase (CsCl type) and martensitic phase with monoclinic lattice or B19' structure [1, 3, 4]. Maximum temperature of martensite transformation is approx. 70 °C for equiatomic composition of NiTi based alloy. When the Ni content in equiatomic composition is reduced, then the temperature of martensitic transformation does not change. If the Ni content increases over 50 at.%, the transformation temperature starts to decrease sharply down to -40 °C for 51 at.% of Ni. If the Ni content increases up to 55 at.%, the transformation temperatures are between -10 °C and 60 °C. This alloy has in comparison with stainless steel an excellent corrosion resistance in salt water or salt spray. The alloy is stable during heat treatment and it is also easy to control its transformation temperature. It is determinant for fabrication of complicated shapes during heat treatment. If the composition is changed, then martensitic transformation can occur at room temperature, which results from SME to pseudoelasticity. NiTi based alloys show fully renewable transformation deformation up to 8 % [1]. **Fig. 1** presents an equilibrium diagram of Ti-Ni, which shows sub-stoichiometric concentrations of the B2 phase for alloys in bi-phase region Ti<sub>2</sub>Ni + NiTi matrix. In the case, when the concentration is higher than stoichiometric, it is necessary to apply quenching of

the B2 phase with consequential annealing at the temperature of 600 °C. This results in precipitation of TiNi<sub>3</sub> or Ti<sub>2</sub>Ni<sub>3</sub>. The Ni content is after precipitation of the phases reduced, while martensitic transformation temperature increases [4].

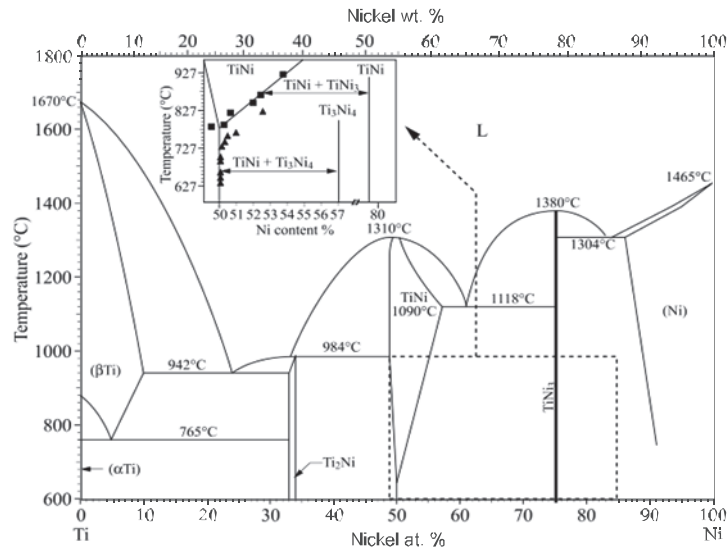


Fig. 1 Equilibrium diagram of Ti-Ni [4]

Precipitation process of alloys rich in Ni at 400 °C enables lenticular precipitation of the Ti<sub>3</sub>Ni<sub>4</sub> phase. On the basis of formation of strain fields from the precipitates of Ti<sub>3</sub>Ni<sub>4</sub>, formation of the *R*-phase between austenitic and martensitic phase can occur. The *R*-phase disappears after annealing at high temperatures [2]. This transition phase created from martensitic transformation through small elongation of the B2 structure in the direction of <111> shows only little hysteresis with small memory effect. If the transition *R*-phase after cooling is created as first, the following transformation scheme will be respected: B2 → *R*-phase → Martensite. First the martensitic transformation will be created, so the *R*-phase will not be visible. After heating a reversible transformation process takes place: Martensite → *R*-phase → B2. The *R*-phase formation is basically influenced by substitution of low at. % of nickel to iron or aluminum by formation of Ti<sub>3</sub>Ni<sub>4</sub> precipitates at aging of the alloy rich in Ni by annealing below the recrystallization temperature after cold forming, by cyclical heat stress or by alloying with the third component. The *R*-phase is used where low hysteresis is needed, or for maintaining the memory effect during small deformation of approx. 1% [3, 4].

If oxygen is present in the alloy as interstitial element, its amount has influence on the temperature of start of martensite transformation, which is linearly decreasing with the increasing oxygen contents. The oxygen solubility in solid solution of NiTi is really small (0.045 at.%) and therefore the alloys containing oxygen above 0.045 at.% are solidifying during cooling of the melt as primary NiTi phase and eutectic mixture of solid solution (NiTi) and oxide (Ti<sub>4</sub>Ni<sub>2</sub>O). Oxygen therefore binds to itself twice as much Ti as Ni in the NiTi phase of the type B2. This results in an increased Ni content in the remaining phase [5]. Reduction of content of gases in the alloy during EBFZM can be difficult to achieve due to creation of thin oxide layer on the surface of the alloy [6].

If the NiTi alloy contains carbon, the temperature of start of martensite transformation also decreases with the increase of carbon contents. Carbon is precipitated in the alloy as a TiC phase and actual Ti contents in the matrix is decreased. At the same time the Ni contents is also increased. Even a small amount of carbon solute in matrix causes decrease of the temperature of start of martensite transformation down to 258 °C. Alloy, containing carbides, has an important effect on yield strength and yield stress. The carbide content in melting alloy depends on the melt temperature and carbide content after melting in graphite crucible; it is in the range approx. from 200 to 500 ppm, which has no influence on the memory effect and properties of the alloy [5].

What concerns the mechanical properties of the NiTi based alloys, these materials are ductile below the transformation temperature and they can be plastically deformed in relatively low strain. Mechanical properties of the NiTi based alloy are shown in **Table 2**. Nitinol has good strength, ductility, and fatigue properties. Tensile strength and yield strength increase with decreasing temperature, and strength-decreases with the increasing temperature up to 327 °C. Decrease of strength is accelerating with the temperature above 377 °C [2, 5]. Elongation is relatively constant up to -100 °C, naturally only if the temperature is reduced really fast. Ductility increases at relatively low rates up to 371 °C, and above this temperature it increases at higher rate. At the temperature above 526 °C the alloy has high ductility, low yield strength and strain rate, and high sensitivity to the change of strain rate. At the temperature of approx. 626 °C ductility is higher by more than 100 % of the initial value. Between the temperatures of approx. 21 - 593 °C the yield strength depends on the strain hardening, which is really rapidly increasing with the temperature. Nitinol has below 21 °C high plasticity due to the martensite transformation. Impact strength of Nitinol is approx. by 25 % higher at -80 °C than at room temperature. Fatigue strength of NiTi is dependent on microstructure and on presence of lattice defects. If NiTi contains only small Ti<sub>3</sub>Ni<sub>4</sub> precipitations, its fatigue strength is lower as compared to the same structure with high dislocation density caused during cold forming [2, 3].

**Table 2** Mechanical properties of equiatomic composition of NiTi based alloys [2]

Tensile strength (MPa)	566 - 966
Yield strength $R_{p0.2}$ (MPa)	227 - 558
Elongation $\epsilon$ (%)	10
Hardness by Rockwell; diamond cone with load of 600 N (HRA)	65 - 68
Impact strength (kJ·m <sup>2</sup> )	32.53
High cycle fatigue at $25 \cdot 10^6$ cycles (MPa)	483

### 1.1. Fabrication of NiTi based alloys

Molten titanium is highly reactive with oxygen, therefore NiTi based alloys are melted in high vacuum or in inert atmosphere. Vacuum induction melting or plasma arc melting are the most frequently used methods. Other used methods are electron beam melting or arc melting in inert atmosphere. The advantage of the first method consists in obtaining of structural homogeneity in the entire cross section of the ingot. It results from induction mixing of the melt. The crucibles used for melting of these alloys are made mainly from graphite, or from calcium oxide (CaO). The aluminum oxide or magnesium oxide are not suitable as material for crucibles, because molten titanium reacts with oxygen included in crucible and it contaminates the melted alloy. If the graphite crucible is used, contamination of the alloy takes place. This contamination is indeed negligible if there is no melting process at the temperature higher than 1450 °C (occurrence of increased carbon contents in the alloy) [5].

Melting by electron beam uses kinetic energy of the beam of incident electrons acting onto melted material. Basic material is melted in the water-cooled copper mould. The alloy solidifies in the lower part of the mould and then it is poured out through the mould bottom. This melting process provides the lowest content of impurities thanks to the refining effect of the high vacuum and high temperature. The composition and homogeneity of the ingot is not adequate, because the alloy is directionally solidifying from the bottom of the mould. Vaporization of the alloy due to high temperature is complicating control of the composition. This method is used for preparation of NiTi based alloys, in which precise processing temperature of martensitic transformation is not needed [5].

The methods of arc melting are divided into two types. The first type uses for melting process a non-fusible electrode, and the second process uses fusible electrode, which is made from the same material as the melt. In the first case tungsten electrode is used and melting process takes place in Cu mould. The final product has

then the shape of a pit. In order to achieve better homogeneity it is necessary to turn around to back solidified pit and remelted. In the second case the electrode is made from the same material as the melt and it melts and falls into the melt [5].

In the case when plasma arc melting is used, the melting is performed by an electron beam emitted from plasma gun (cathode). Electron emitting is milder in comparison with high-voltage electron beam melting or arc melting in an inert atmosphere. The result is lower loss of components in the alloy. The alloy is then more homogeneous even in case of use of the water-cooled Cu crucible [5].

## 1.2. Forming of NiTi based alloys

The alloy is commercially produced in numerous variants in the form of wires, plates, rods or even tubes and sheets. Although the alloy has good forming properties at the temperature of 526 °C, the optimal temperature for hot forming is approx. 850 °C. During the hot forming light surface oxidation can occur. Extrusion, rolling or stamping at the temperature range from 600 to 900 °C can be used for hot forming of Nitinol. The final rolling to strips or wire drawing can be made at the temperature of approx. 400 °C [2, 5]. In comparison with hot forming process the cold forming process is fully dependent on the composition. Formability of these materials decreases with the increase of the Ni content, especially when Ni content is higher than 51 at. %. It is result of higher strain hardening. Yield strength for annealed NiTi based alloy is not higher than 100 MPa (similarly as for the soft annealed Cu or Al). If is NiTi annealed wire is deformed its tensile strength increased at ~10 % of strain and at ~40 % or strain is 1000 MPa. In the case of cold wire drawing the tensile strength is higher than 1500 MPa [5].

## 2. EXPERIMENTAL PROCEDURES

For experimental determination of structural characteristic a NiTi based alloy was created with equiatomic composition of its components. Cathode nickel with purity 4N and shaped rolled titanium of purity 2N8 were used as the input materials. The content of nickel was 50.85 at. % and content of titanium was 49.15 at. %. The total amount of the alloy was 705 g. The original alloy was prepared by vacuum induction melting process in graphite crucible. The output sample was 225 mm long and had diameter of 20 mm. Hot swaging was then applied to the alloy without inert atmosphere. Four reductions were applied and the alloy was annealed between individual steps of swaging. The final diameter was 10 mm and length was 350 mm. The swaging was followed by Electron Beam Floating Zone Melting (EBFZM) where a narrow zone was melted using electron emission. After that the melting zone passed through the required length of the NiTi rod. This technology is also suitable for preparation of single crystals made of refractory metals [7]. The alloy was remelted by a single passage through the melting zone. The length of the remelted rod was 150 mm. Travel speed of the molten zone was 3 mm/min. The average value of vacuum was  $8.3 \cdot 10^{-4}$  Pa, cathode voltage was 6 kV, current cathode was from 13.86 A to 14 A and cathode emission was from 35 mA at the beginning of the rod to 29 mA at the end of melting.

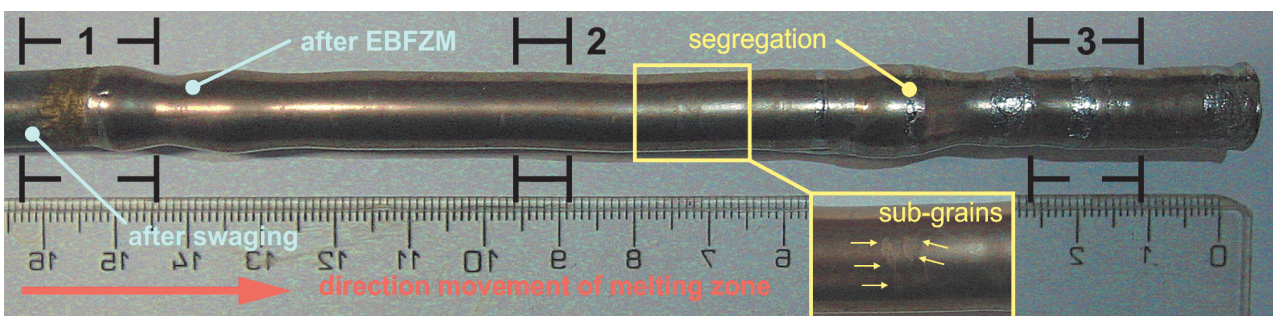


**Fig. 2** Sample of NiTi based alloy after EBFZM

After EBFZM three samples were cut from the alloy for metallographic analysis. The sample 1 was taken from the transition zone between the formed and remelted area, it was a longitudinal section. Sample 2 was taken from the centre of the remelted rod, it was a cross section, and the last sample 3 was taken as longitudinal section (**Fig. 2**).

The samples were subjected to metallographic analysis with uses of optical microscope. All the samples were ground using abrasive paper discs with SiC. Polishing was applied using water suspension of Al<sub>2</sub>O<sub>3</sub>. Microstructure was developed by an etching agent 1HF: 4HNO<sub>3</sub>: 5H<sub>2</sub>O and observation of the microstructure and taking pictures of it was realised on the microscope Olympus GX 51, equipped with the digital camera DP 12. The samples were then taken for EDX analysis and the last analysis consisted in determination of interstitial elements in the alloy (O<sub>2</sub>, N<sub>2</sub> a C). The interstitial elements were analysed by elementary analysis (EA) using the ELTRA ONH - 2000 and ELTRA CS - 2000 analysers on the sample 2.

### 3. RESULTS AND DISCUSSIONS

On the surface of the NiTi rod remelted by EBFZM macro-segregation was detected, which was seen only in the second part of the rod. It was result of redistribution of impurities and elements during EBFZM. Sub-grains were also seen on the surface of the remelted rod, see **Fig. .** This fact was confirmed by the cross section of the sample 2. In **Chyba! Nenalezen zdroj odkazů.** the microstructures of NiTi alloy are shown. **Chyba! Nenalezen zdroj odkazů.** a) shows really clear transition between the swaging part and EBFZM part of the sample. After EBFZM a precipitated Ti<sub>2</sub>Ni phase and carbide TiC were found in the microstructure, which got into the alloy from the graphite crucible.

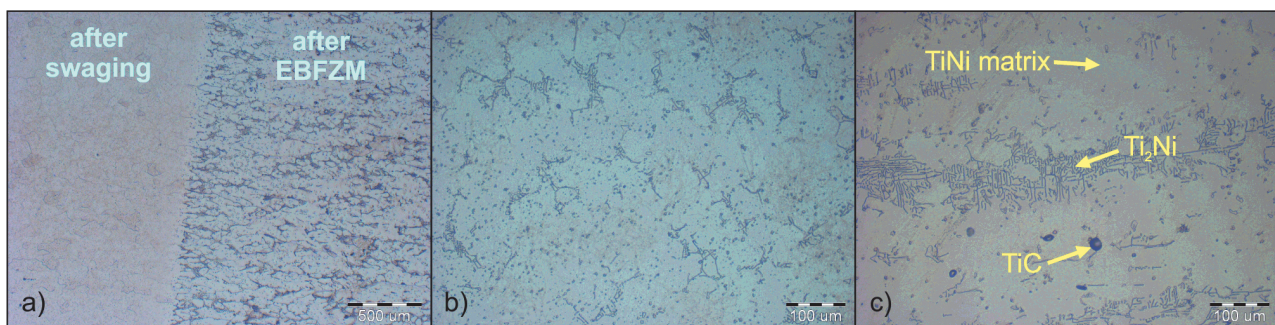


**Fig. 3** Microstructure of NiTi based alloy a) sample 1, longitudinal section, scale 500 μm; b) sample 2, cross section, scale 100 μm; c) sample 3, longitudinal section, scale 100 μm

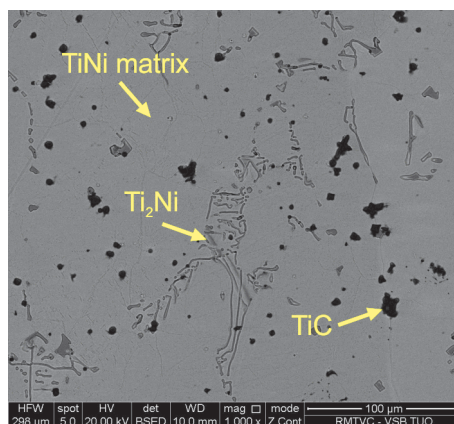


**Fig. 4** Microstructure of NiTi based alloy, longitudinal section of the sample 3

EDX analysis confirmed average composition of the alloy in all the samples, which was 50.55 at.% of Ni and 49.33 at.% of Ti. Composition of the present phases is given in **Table 3**. **Fig. 4** shows microstructures after EDX analysis.

**Table 3** Average composition of NiTi based alloy phases after EDX analysis (at.%)

Phase	Ti	Ni	C
NiTi matrix	49	51	—
Ti <sub>2</sub> Ni	66.19	33.81	—
TiC	58.07	—	41.93

The results of gas analysis after EBFZM are presented in **Table 4**. In vacuum induction melting in comparison with EBFZM is the gas content higher than after EBFZM. It could be expected that gas content will be lower because EBFZM process runs under high vacuum ( $10^{-4}$  Pa) but it is not so. During application of EBFZM no escape of gases from the melt by the sputter droplets from the melt was visible.

**Table 4** Analysis of interstitial elements in NiTi based alloy after EBFZM (wt.%)

Technology	O <sub>2</sub>	N <sub>2</sub>	C
Vacuum induction melting	0.065	0.004	0.039
EBFZM	0.145	0.037	0.108

#### 4. CONCLUSIONS

In the second part of the rod macro-segregations were seen in the structure after applied EBFZM. Sub-grains were distinctly seen inside the alloy structure. During EBFZM no significant changes of composition along the longitudinal section of the rod took place. It was found that the gas content in the NiTi based alloy was higher after the applied EBFZM. Higher content of gases in the alloy might have caused creation of thin oxide layer on the surface of rod during swaging without protection of inert atmosphere. It will be necessary to make other experiments in order to explain higher gas content in the NiTi based alloys.

#### ACKNOWLEDGEMENTS

*This paper was created at the Faculty of Metallurgy and Materials Engineering within the Project No. LO1203 "Regional Materials Science and Technology Centre - Feasibility Program" funded by the Ministry of Education, Youth and Sports of the Czech Republic.*

#### REFERENCES

- [5] LAGOUDAS D.C. Shape Memory Alloys: Modeling and Engineering Applications. New York: Springer Science+Business Media, LLC, 2010, 436 p. ISBN 978-0-387-47684-1.
- [6] EVERHARD J.L. Engineering Properties of Nickel and Nickel Alloys. New Jersey: Springer, 2012, 229 p. ISBN 978-1-4684-1886-6.
- [7] YAMAUCHI K., et al. Shape Memory and Superelastic Alloys: Applications and Technologies. Cambridge: Woodhead Publishing Limited, 2011, 232 p. ISBN 978-1-84569-707-5.
- [8] LEXCELLENT C. Shape-Memory Alloys Handbook. Croydon (Great Britain): ISTE Ltd and John Wiley & Sons, Inc. 2013, 400 p. ISBN 978-1-84821-434-7.
- [9] OTSUKA K., WAYMAN, C.M. Shape Memory Materials. Cambridge: Cambridge University Press, 1998, 298 p. ISBN 0-52-1-44487-X.
- [10] SZURMAN I., KOCICH R., KURSA M. Shape Memory Alloys: Fabrication and processing. Herstellung (Německo): LAP LAMBERT Academic Publishing, 2012, 102 p. ISBN 978-3-848-2535-8.
- [11] SKOTNICOVÁ K., KIRILLOVA V.M., DRÁPALA J., BURKHANOV G.S., KUZ'MISHEV V.A., SDOBYREV V.V., DEMENTYEV V.A., ABRAMOV N.N. Preparation and investigation of structural parameters of single crystals of low-alloyed alloys on the base of tungsten and molybdenum. Advanced Engineering Materials, Wiley-VCH, Vol. 15, No. 10, 2013, pp. 927-934, ISSN 1438-1656.